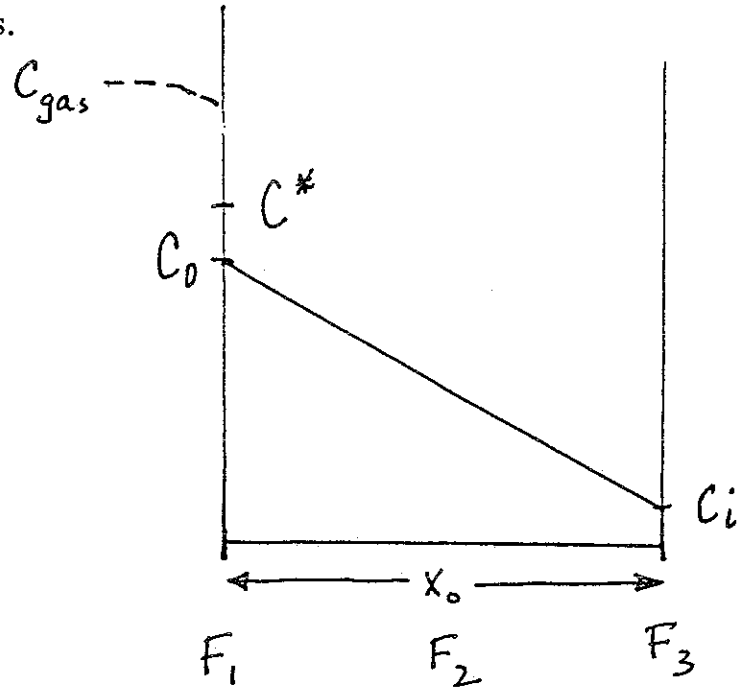


# Oxidation

Oxidation occurs via the reaction of an oxidant (commonly  $O_2$  or  $H_2O$ ) at the Si-SiO<sub>2</sub> interface.

This requires a number of steps.

1. Transport of oxidant in gas phase to surface and adsorption there.
2. Diffusion of oxidant through oxide film.
3. Reaction of oxidant with silicon substrate.



We can model each of these processes.

For gas-phase transport and adsorption, we can define  $C^*$  to be the concentration of oxidant in the oxide at equilibrium with the concentration in the gas phase. The relationship is given by a segregation coefficient:

$$C^* = m_{\text{oxide/gas}} C_{\text{gas}} = K_{HP} \quad (1)$$

More commonly, the partial pressure  $p$ , rather than the volume concentration within the gas is specified and the segregation coefficient is replaced by Henry's constant  $K_H$  (just a change of units).

This relationship implies that the adsorption is a first order reaction, that is that one gas molecule is required to produce one molecule within the oxide.

The rate of adsorption can be written as

$$F_1 = h(C^* - C_0) \quad (2)$$

where  $C_0$  is the concentration of the oxidant in the oxide near the surface of the oxide.  $h$  is the rate constant for the reaction and depends on both gas-phase kinetics as well as adsorption kinetics.

Once within the oxide, the oxidant diffuses. Ignoring any reaction within the oxide, the continuity equation is:

$$\frac{\partial C}{\partial t} = D \frac{\partial^2 C}{\partial x^2} \quad (3)$$

where  $D$  is the effective diffusivity of the oxidant within the oxide.

The effective oxidant diffusivity is fast enough relative to the oxidation rate, that the distribution of oxidant at any time can be approximated by the distribution that would exist if the oxide thickness was not increasing. Thus we can assume a quasi-steady-state for the oxidant distribution ( $\partial/\partial t \Rightarrow 0$ ).

The solution to the continuity equation is then

$$C = C_0 - \frac{C_0 - C_i}{x_0} x \quad (4)$$

where  $C_i$  is the oxidant concentration at the Si-SiO<sub>2</sub> interface and  $x_0$  is the oxide thickness.

The flux through the oxide is given by Fick's Law:

$$F_2 = -D \frac{\partial C}{\partial x} = D \frac{C_0 - C_i}{x_0} \quad (5)$$

Finally the reaction at the interface is assumed to be a first-order reaction and the reverse reaction is neglected since  $\text{SiO}_2$  is very stable.

$$F_3 = k_s C_i \quad (6)$$

where  $k_s$  is the rate of the interface reaction.

The fluxes of oxidant at the two interfaces of the oxide have to balance so:

$$F_1 = F_2 = F_3 \quad (7)$$

Thus, we have two equations and two unknowns ( $C_0$  and  $C_i$ ).

Solving for  $C_i$  by applying  $F_1 = F_2$  and  $F_2 = F_3$

$$C_i = \frac{DC^*/k_s}{x_o + D(1/h + 1/k_s)} \quad (8)$$

All of the oxidant flowing through the system ends up as oxide, so the oxidation rate can be written in terms of any of the fluxes. Using  $F_3$ ,

$$\frac{dx_o}{dt} = \frac{1}{N} k_s C_i = \frac{DC^*/N}{x_o + D(1/h + 1/k_s)} \quad (9)$$

where  $N$  is the number of oxidant molecules required to produce a unit volume of oxide. For an oxidant with 2 oxygen atoms (like  $\text{O}_2$ ),  $1/N$  is just the molecular volume of  $\text{SiO}_2$ .

The oxidation rate is commonly written as

$$\frac{dx_o}{dt} = \frac{B}{2x_o + A} \quad (10)$$

where

$$B = 2DC^*/N \quad (11)$$

and

$$A = 2D(1/h + 1/k_s) \quad (12)$$

To find the time-dependence of the oxide thickness, we can rearrange and integrate:

$$\int_0^t B dt = \int_{x_i}^{x_o} (2x_o + A) dx_o \quad (13)$$

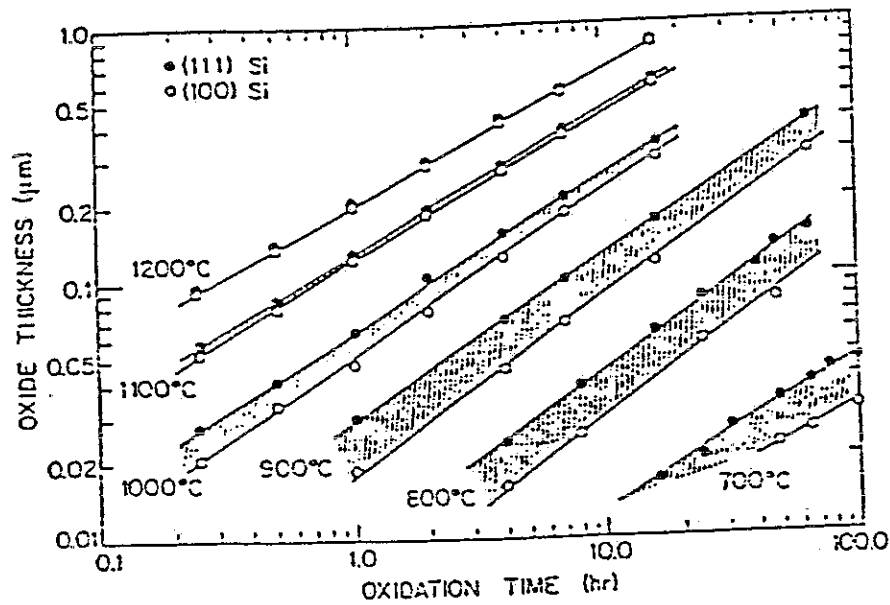
$$t = \frac{x_o^2 - x_i^2}{B} + \frac{x_o - x_i}{B/A} \quad (14)$$

$$t + \tau = \frac{x_o^2}{B} + \frac{x_o}{B/A} \quad (15)$$

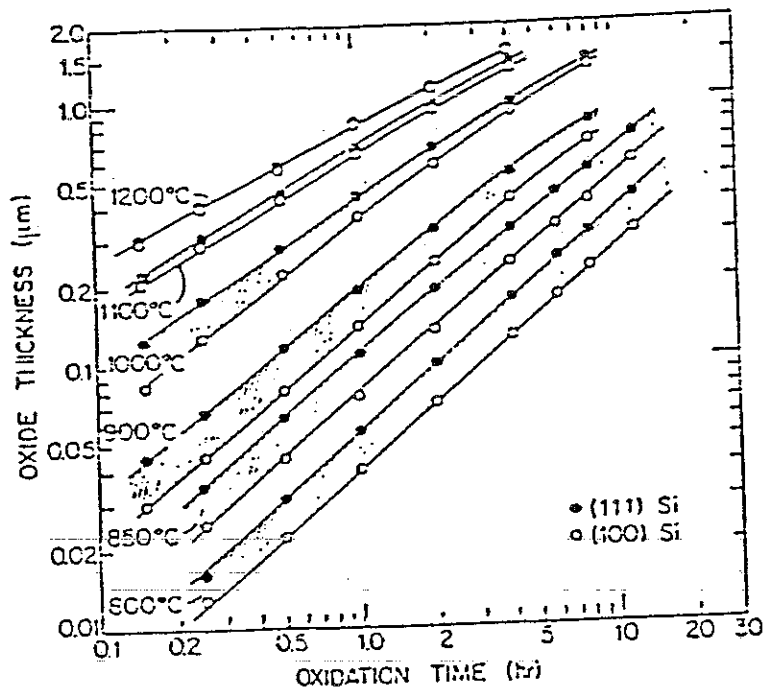
where  $\tau = (x_i^2 + Ax_i)/B$ .

These equations can also be solved for the oxide thickness as a function of time.

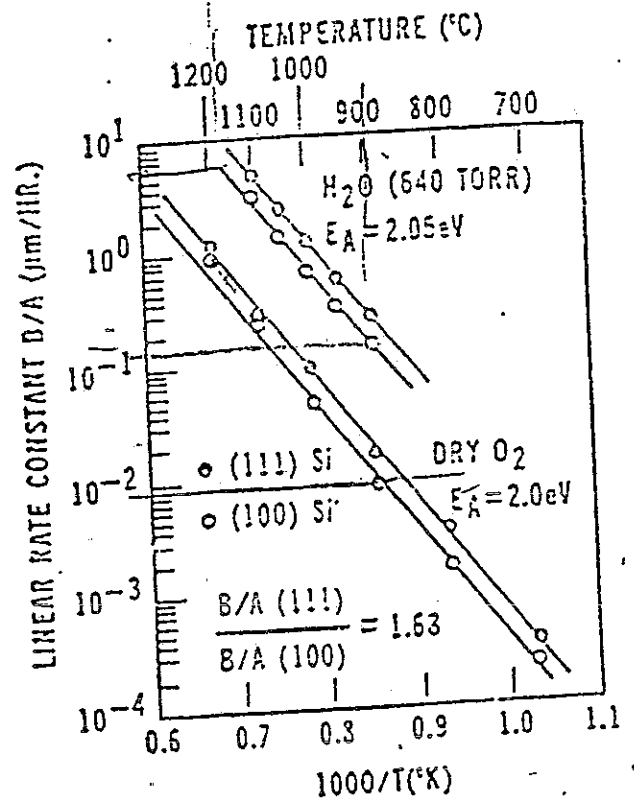
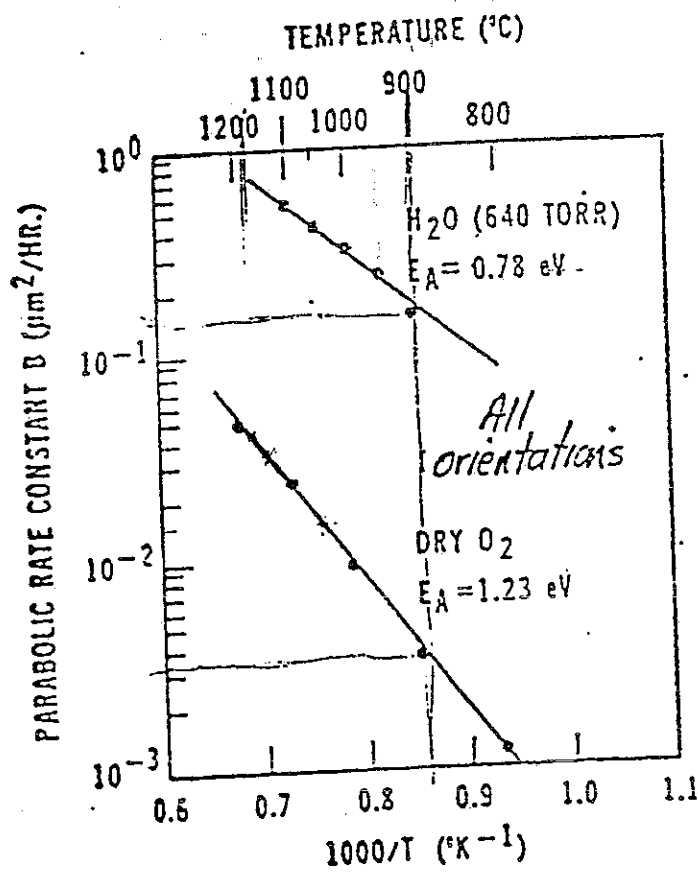
dry O<sub>2</sub>



steam



$B$  and  $B/A$  are called, respectively the parabolic and linear rate constants and can be approximated by Arrhenius expressions.



For large oxide thicknesses ( $x_o \gg A/2$ ),  $x_o \cong \sqrt{Bt}$ .

Under these circumstances, the oxide growth is limited by the diffusion through the oxide as is clear from the fact that  $B$  is proportional to the effective oxidant diffusivity. As the oxide thickness grows, the flux through the oxide drops, reducing the oxidation rate ( $dx_o/dt \cong B/2x_o$ ).

For thinner oxides ( $x_o \ll A/2$ ), the oxidation rate is limited by the reactions and the oxidation rate is approximately constant ( $dx_o/dt \cong B/A$  and  $x_o - x_i \cong (B/A)t$ ).

It has been shown that  $h \gg k_s$  so that the linear rate constant is

$$\frac{B}{A} = \frac{C^*/N}{(1/h + 1/k_s)} = \frac{C^*k_s}{N} \quad (16)$$

which is proportional to the interface reaction rate  $k_s$ .

The linear rate constant depends on the substrate orientation, with the oxidation rate being largest for  $\langle 100 \rangle$  substrates and smallest for  $\langle 111 \rangle$ . The relative rates are nearly constant over temperature

$$\left(\frac{B}{A}\right)_{\langle 100 \rangle} = 1.68 \left(\frac{B}{A}\right)_{\langle 111 \rangle} \quad (17)$$

The differences in linear rate constant between the different orientations has been explained based on differences in the density and orientation of bonds at the interface.

This analysis was first done for oxidation by Deal and Grove in the late 60s and is often termed the Deal-Grove or linear-parabolic model. The model has been very successful for many years in modeling oxidation kinetics, but it does have a few limitations.

### Partial pressure dependence

In the Deal-Grove model, both the linear and parabolic rate constants are proportional to the solubility  $C^*$  and thus the oxidant partial pressure  $p$ .

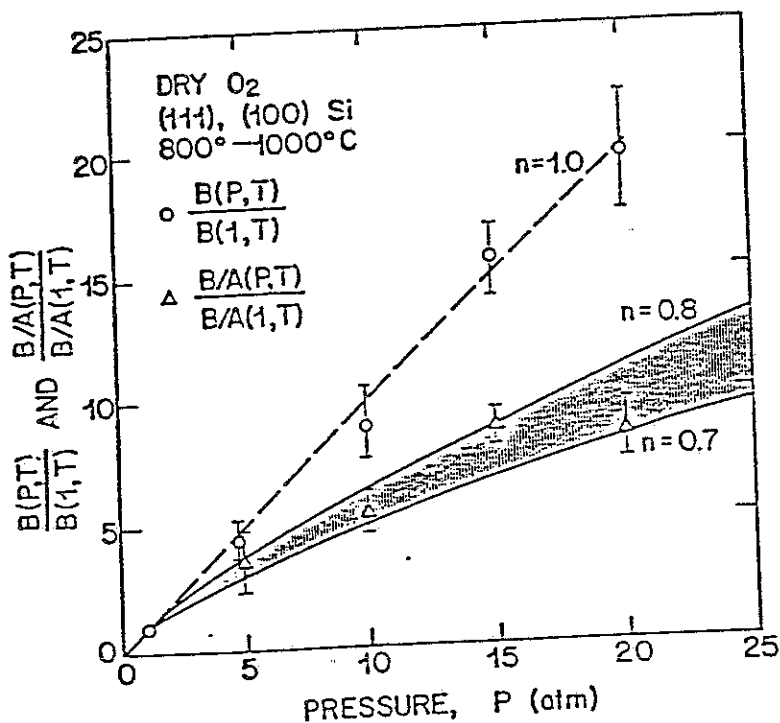
For steam oxidation, this agrees with experiment as  $B$  and  $B/A$  are proportional to  $p_{\text{H}_2\text{O}}$ .

This confirms the assumption that the diffusing and reacting species have the same number of oxygen atoms as in the gas phase (first-order reactions).

For oxidation in dry  $O_2$ , the parabolic rate constant depends linearly on  $p_{O_2}$ , which confirms that the primary diffusing species contains two oxygen atoms. However, the linear rate constant manifests a sublinear dependence on  $p_{O_2}$ .

$$\left(\frac{B}{A}\right)_{O_2} \propto p_{O_2}^n$$

$$0.5 < n < 1.0$$



This can be explained by assuming that an oxidant species with a single oxygen atom has an important role in the interface reaction.

Consider



$$C_O^2 = K(T)C_{O_2} \quad C_O = K(T)^{1/2}C_{O_2}^{1/2} \quad (19)$$

Thus if the reaction involving the atomic oxygen dominates, the linear rate constant would be proportional to  $p_{O_2}^{1/2}$ , while if the molecular species dominated the interface reaction,  $B/A \propto p_{O_2}$ . If both reactions are important, then the experimentally-observed dependence results ( $0.5 < n < 1.0$ )

The modeling suggests that the numbers of atomic species are far fewer than the numbers of molecular species and are thus negligible in the diffusion flux, but the atomic species provide an important path for oxidation since they are much more reactive.

## Thin oxide kinetics

When modeling oxidation kinetics in dry  $O_2$  using the linear-parabolic model, the values of  $x_i$  required to match the data are on the order of 100-200 Å, rather than the initial thickness observed experimentally of about 20 Å.

In the thin regime ( $< 400$  Å), the oxide thickness as measured by ellipsometry increases more rapidly than predicted by the linear-parabolic model.

There are many competing models to explain this behavior:

- Alternate paths such as micropores
- Multiple diffusing species
- Electric field effects
- Empirical corrections (SUPREM IV)

$$\frac{dx_o}{dt} = \frac{B}{2x_o + A} + Ke^{-x/L} \quad (20)$$

TEM vs. Ellipsometry

Oxide thicknesses measured by TEM manifest linear growth for thin oxides which suggests that the apparent faster growth of thin oxides may simply be a measurement artifact.

If the interface roughness increases during the early stages of oxidation (as observed experimentally), this would appear to ellipsometry as a greater optical thickness.

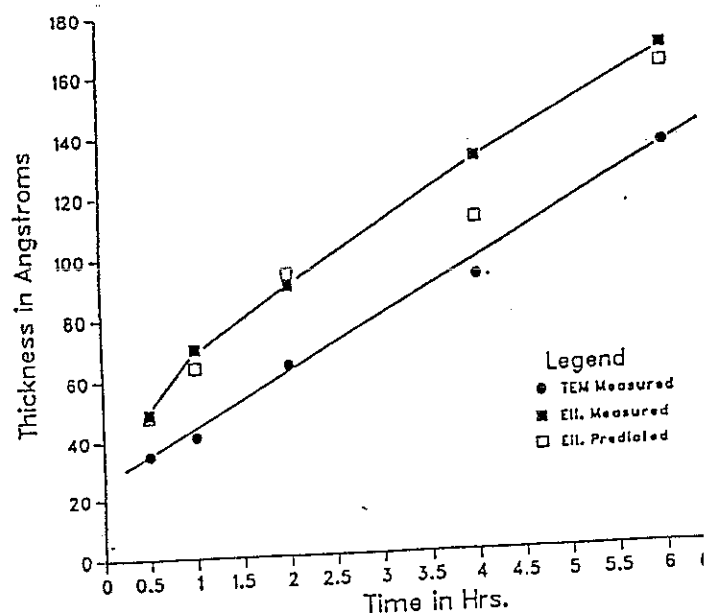
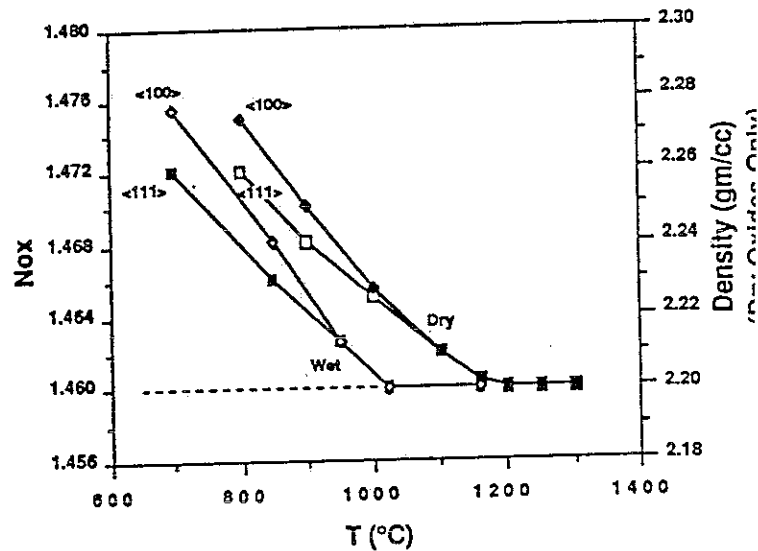
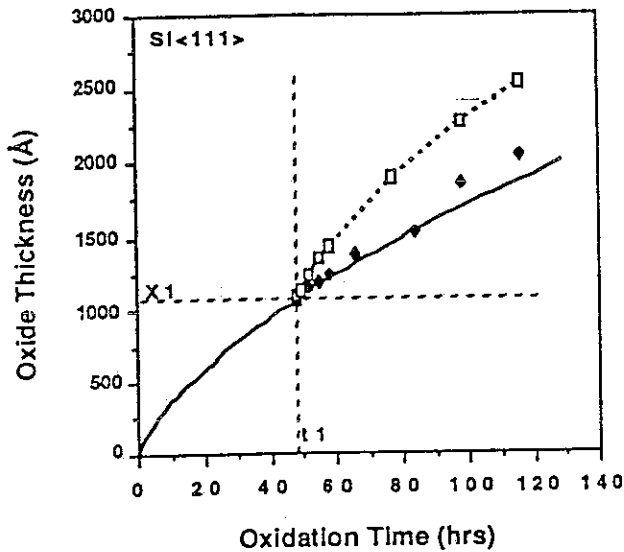


Figure 2: Comparison of measured and calculated oxide thickness. Data from Carim and Sinclair



## Thermal history effects

If two oxides of the same thickness, but grown at different temperatures are subsequently oxidized at a lower temperature, the oxidation kinetics will vary strongly, with the oxide grown at the higher temperature (or in steam) oxidizing faster.



-□- Subsequent Oxidation  
of 1180°C-Grown SiO<sub>2</sub>  
at 800°C

● Subsequent Oxidation  
of 800°C-Grown SiO<sub>2</sub>  
at 800°C

— Normal Oxidation  
at 800°C:  
B = 795 Å<sup>2</sup>/min  
B/A = 0.58 Å/min  
B1 = 40 Å<sup>2</sup>/min

The differences between oxides grown at different temperatures can be observed directly as lower temperature oxides have a higher refractive index, which implies that they are denser.

Since oxidant diffusion is interstitial, diffusivity can be expected to drop with increasing oxide density.

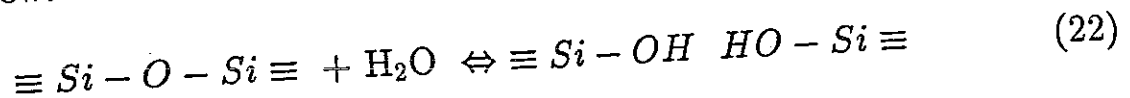
Annealing at high temperature can also be used to reduce the refractive index and increase the rate of subsequent oxidation.

The increased density of oxides grown at low temperatures can be explained by noting that the oxidation reaction requires substantial expansion since

$$\Omega_{\text{SiO}_2} \cong 2.2\Omega_{\text{Si}} \quad (21)$$

Expansion in the plane of the interface is constrained by the connections between the oxide and the substrate, while upward expansion depends on viscous flow, which is much faster at higher temperatures.

The differences between dry and steam oxides can be accounted for by noting that  $\text{H}_2\text{O}$  can act as a network breaker, reducing viscosity and aiding relaxation via viscous flow.



### Oxidation of heavily-doped material

It has been observed experimentally that oxidation of heavily-doped material is increased over that of lightly-doped substrates.

The behavior is different for p-type (boron-doped) material than for n-type substrates.

For heavily boron doped material, the main change in the kinetics appears in the parabolic rate constant. This is easily explained since boron segregates to the oxide and the presence of a large fraction of boron in the oxide modifies (weakens) the network, increasing the oxidant diffusivity and solubility.

In contrast, for heavily donor doped material, the main change is in the linear rate constant and is correlated to the electron concentration:

$$\frac{B}{A} = \left(\frac{B}{A}\right)_i \left[1 + K \frac{n - n_i}{n_i}\right] \quad (23)$$

There are two possible explanations for this behavior:

- It has been proposed by Ho and Plummer that the increased oxidation rate is due to the increase in the concentration of negatively-charged vacancies, which provides oxidation sites.
- The electrons may directly facilitate the breaking of the oxygen-oxygen or silicon-silicon bonds as required for the interface reaction.

### Oxidation in chlorine-containing ambients

Often, chlorine (or more recently fluorine) species such as HCl or TCA ( $C_2H_3Cl_3$ ) are added to the dry  $O_2$  ambients in order to:

- Getter metallic impurities
- Immobilize sodium ions
- Improve dielectric strength

In addition, the addition of chlorine

- Increases the oxidation rate
- Results in chlorine incorporation near the Si-SiO<sub>2</sub> interface.

These effects can be attributed to

- Generation of H<sub>2</sub>O
- Alternative oxidation path due to reaction of chlorine at interface.
- Reduced viscosity due to network termination by Cl (like steam).

# Oxidation of Non-Planar Structures

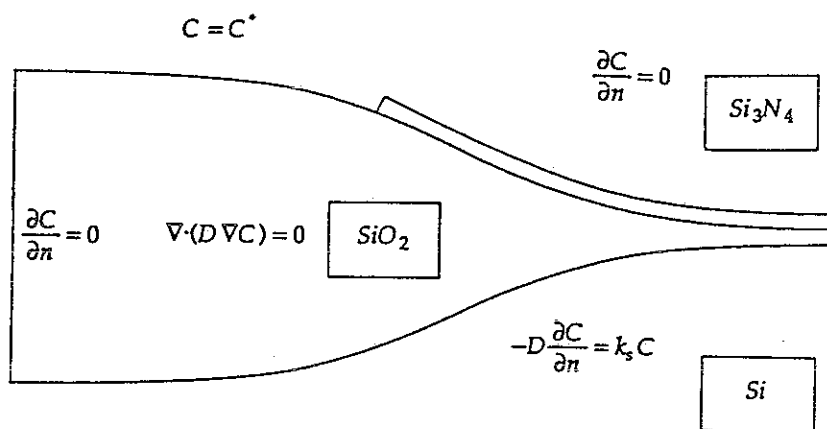
So far, we have only considered oxidation in planar structures (1D). In non-planar (2D or 3D) structures, the analysis is more complicated.

A particular important example is the LOCOS (LOCAl Oxidation of Silicon) process used for device isolation.

In the LOCOS process, a portion of the substrate is protected from oxidation by a nitride layer over a thin pad oxide.

During heating in an oxidizing ambient, oxide grows not only in the exposed regions, but also under the edges of the nitride due to lateral diffusion.

The resulting structure is often termed a "bird's beak" due to the shape.



A direct extension of our 1D analysis would have us solve the oxidant diffusion equation:

$$\frac{\partial C_{\text{H}_2\text{O}}}{\partial t} = \nabla \cdot D_{\text{H}_2\text{O}} \nabla C_{\text{H}_2\text{O}} (= 0 \text{ in steady state}) \quad (1)$$

with boundary conditions

$$C_{\text{H}_2\text{O}} = K_{\text{HP}} P_{\text{H}_2\text{O}} \quad \text{at gas/oxide interface} \quad (2)$$

$$D_{\text{H}_2\text{O}} \frac{\partial C_{\text{H}_2\text{O}}}{\partial x} = k C_{\text{H}_2\text{O}} \quad \text{at oxide/silicon interface} \quad (3)$$

$$D_{\text{H}_2\text{O}} \frac{\partial C_{\text{H}_2\text{O}}}{\partial x} = 0 \quad \text{at oxide/nitride interface} \quad (4)$$

Note that the nitride will be pushed up at the edges due to oxide growth underneath. SUPREM IV can model this system assuming that oxide growth is strictly vertical (method vertical).

However, the structures which are observed experimentally differ substantially from the solutions to this system whenever the structure diverges significantly from planar.

What is ignored in the simple analysis, is the viscous flow of oxide and the resistance to bending of the nitride layer.

For a solid, Newton's second law ( $F = ma$ ) is written:

$$\sum_j \frac{\partial \sigma_{ij}}{\partial x_j} + B_i = \rho a_i \quad (5)$$

where  $\rho$  is the density,  $a_i$  is the acceleration in direction  $i$ ,  $\sigma_{ij}$  are the elements of the stress tensor (force per unit area in  $j$  direction on a plane cut normal to the  $i$  directions),  $x_j$  is distance in direction  $j$ , and  $B_i$  is any forces on the body (i.e., gravity).

For oxidation, acceleration and gravity are negligible so

$$\sum_j \frac{\partial \sigma_{ij}}{\partial x_j} = 0 \quad (6)$$

which simply says that all the forces on a small block of material cancel.

Strain is the relative atom displacement and is given by

$$\epsilon_{ij} = \frac{1}{2} \left( \frac{\partial d_i}{\partial x_j} + \frac{\partial d_j}{\partial x_i} \right) \quad (7)$$

where, as for stresses, for  $i = j$ , the strains are termed axial and for  $i \neq j$  the strains are shear.

To complete the analysis, it is necessary to define the relationship between stress and strain. This relation is known as the constitutive relation.

The simplest example is linear elastic deformation:

$$\epsilon_{ii} = \sum_j M_{ij} \sigma_{jj} \quad (8)$$

where  $M_{ij} = 1/E$  ( $E$  is Young's modulus) for  $i = j$  and  $M_{ij} = -\nu/E$  ( $\nu$  is the Poisson ratio) for  $i \neq j$ , and

$$\epsilon_{ij} = \frac{2(1+\nu)}{E} \sigma_{ij} \quad (9)$$

for  $i \neq j$ . However, this is only valid for small deformations ( $< 1\%$  for  $\text{SiO}_2$ ) and actual deformations are on the order of 40%.

The opposite extreme, which is more appropriate for  $\text{SiO}_2$  at oxidation temperatures is purely viscous behavior where the stress depends on the time-derivative of the strain.

$$\sigma_{ij} = 2\mu \frac{\partial \epsilon_{ij}}{\partial t} - p\delta_{ij} \quad (10)$$

where  $\mu$  is the viscosity and  $p$  is the hydrostatic pressure.

For viscous flow of an incompressible fluid (method viscous),

$$\nabla \cdot v = 0 \quad (11)$$

where  $v$  is the velocity and

$$\frac{\partial \epsilon_{ij}}{\partial t} = \frac{1}{2} \left( \frac{\partial v_i}{\partial x_j} + \frac{\partial v_j}{\partial x_i} \right) \quad (12)$$

These conditions in addition to Equation (6) results in differential equations for  $v_x$ ,  $v_y$  and  $p$  within the oxide. The parameters (Young's modulus, Poisson ratio and viscosity as a function of temperature) can be set in SUPREM IV using the material statement.

The boundary conditions are defined by the velocity (growth rate) at the interface.

It is more computationally efficient to allow oxide to be “slightly compressible” (method compress) so that

$$-p = B \cdot \nabla v \quad (13)$$

with  $B$  taken to be very large to approximate incompressibility so that only the differential equations for  $v_x$  and  $v_y$  need to be solved. The disadvantage of this method is that although the resulting velocity fields are nearly the same, it is not possible to accurately calculate stresses.

To this point, we have considered linear viscous flow, that is  $\mu$  is constant. However, due to the very large stresses and deformations, it is believed that the viscosity depends on the stress,

$$\mu = \mu_0 \frac{\tau/\sigma_c}{\sinh(\tau/\sigma_c)} \quad (14)$$

where  $\sigma_c = kT/V_c$  is a critical stress ( $V_c \sim 200 \text{ \AA}^3$  is an activation volume) and

$$\tau = \frac{1}{2} \sqrt{(\sigma_{xx} - \sigma_{yy})^2 + 4\sigma_{xy}^2} \quad (15)$$

For large stresses on the order of  $\sigma_c$  and above, the viscosity is greatly reduced from its value for small stresses  $\mu_0$ .

The stress has two implications.

- Excessive stresses can cause defect generation in the silicon (e.g., dislocations), degrading device behavior.

- Oxidant diffusion in the oxide and reaction rate are functions of stress.

$$\frac{D}{D_0} = \exp\left(-\frac{pV_d}{kT}\right) \quad (16)$$

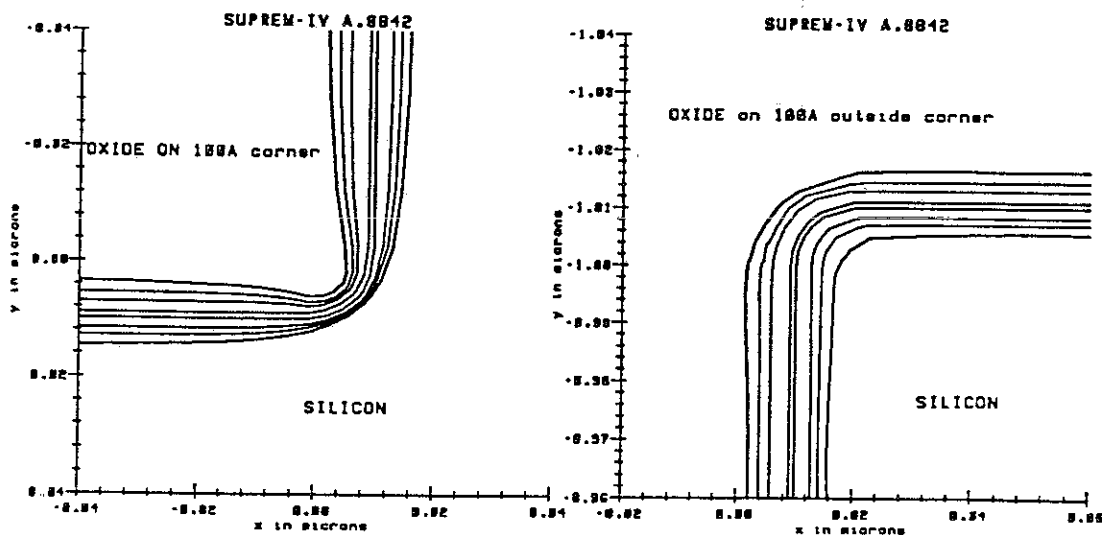
where  $V_d \sim 20 \text{ \AA}^3$  is the activation volume for diffusion. Another parameter 'Dlim' prevents the diffusivity from increasing strongly under tension.

$$\frac{k}{k_0} = \exp\left(-\frac{\sigma_n V_r + \sigma_t V_t}{kT}\right) \quad (17)$$

where  $V_r \sim 25 \text{ \AA}^3$  and  $V_t$  are the activation volumes for the reaction due to normal  $\sigma_n$  and tangential  $\sigma_t$  stress, respectively.

It is only possible to accurately include stress-dependent behavior (by using 'method stress.dep') when using the 'method viscous' since only then are accurate stress values available.

Stress-dependent oxidation is particularly important when modeling corners such as are present during oxidation of trenches. Due to the resulting compression, inner corners tend to result in greatly reduced oxidation, while outer corners show slightly enhanced rates.

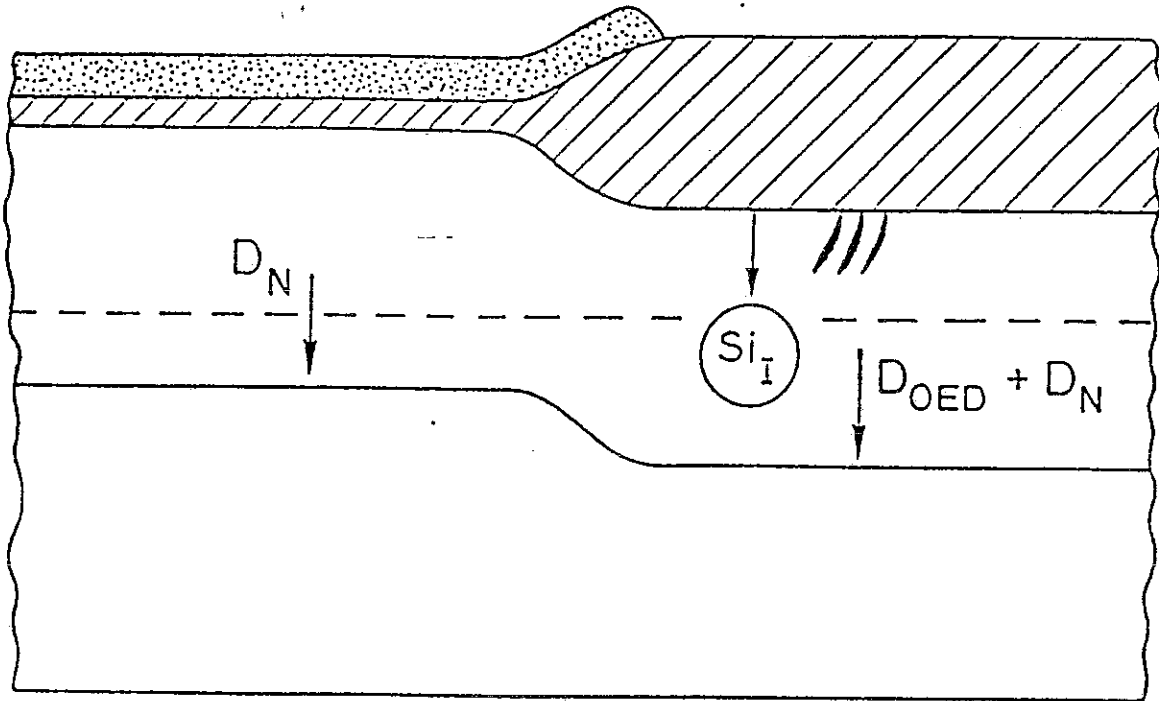


(a) Inside Corner

(b) Outside Corner



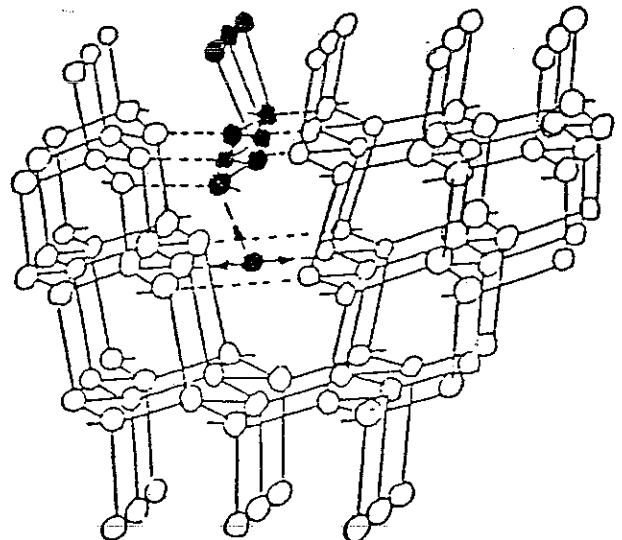
# Effect of Oxidation on Point Defect Concentrations



In the silicon under oxidizing regions, several effects are observed including:

- Enhanced diffusion of P, B and As and retarded diffusion of Sb.
- Growth of interstitial-type stacking faults.

A stacking fault is an extra partial plane of atoms that can grow by adding interstitials or emitting vacancies and shrink by adding vacancies or emitting interstitials



We can note that:

- Enhanced diffusion implies an interstitial or vacancy supersaturation.
- Retarded diffusion implies an interstitial or vacancy undersaturation.
- Stacking fault growth implies an interstitial supersaturation and/or a vacancy undersaturation.

Thus, we can conclude that

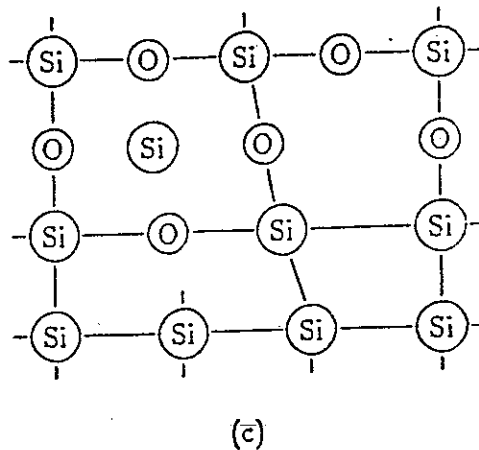
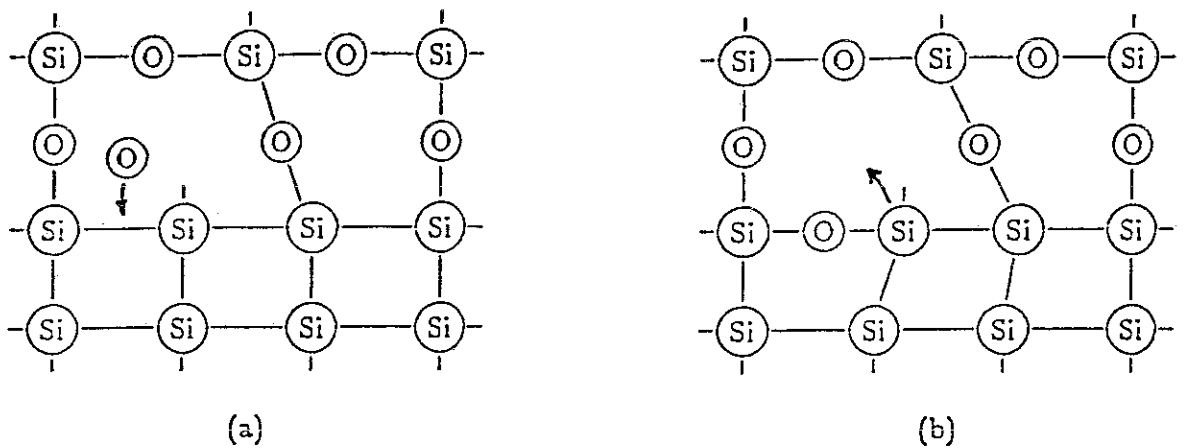
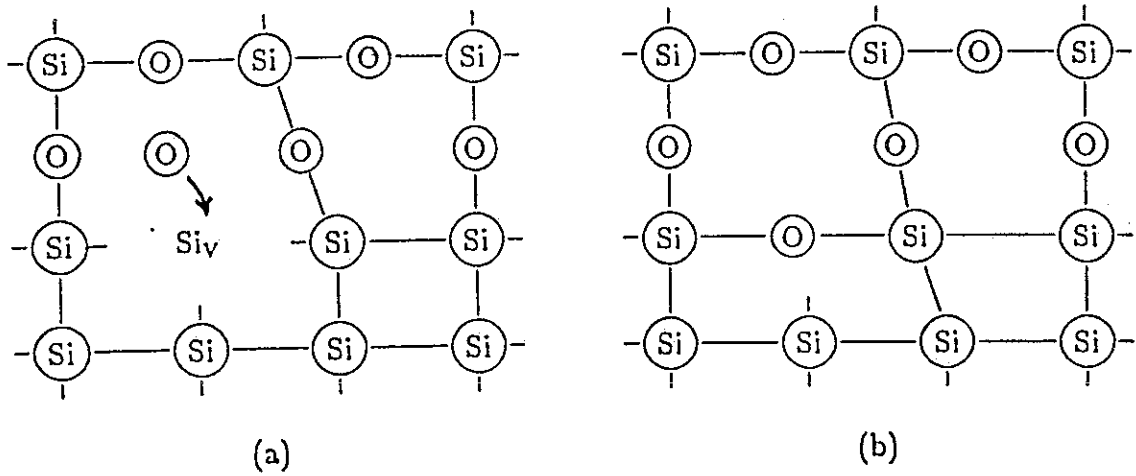
- Oxidation results in an interstitial supersaturation and a vacancy undersaturation.
- Antimony diffuses primarily with vacancies.
- Phosphorus, boron and arsenic have a significant interstitial component to their diffusion.

It is reasonable that the oxidation process causes an interstitial supersaturation or vacancy undersaturation because of the volume expansion required ( $\Omega_{\text{SiO}_2} \cong 2.2\Omega_{\text{Si}}$ ).

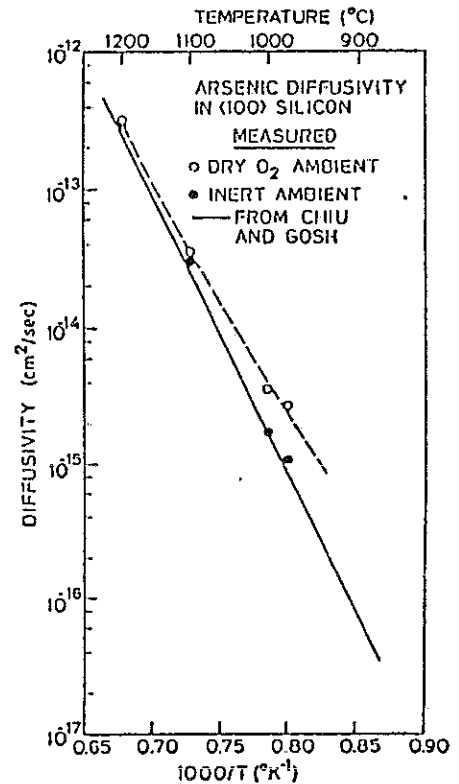
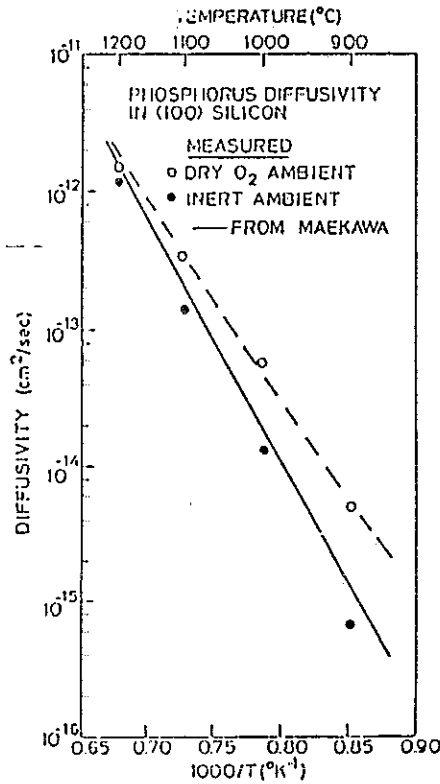
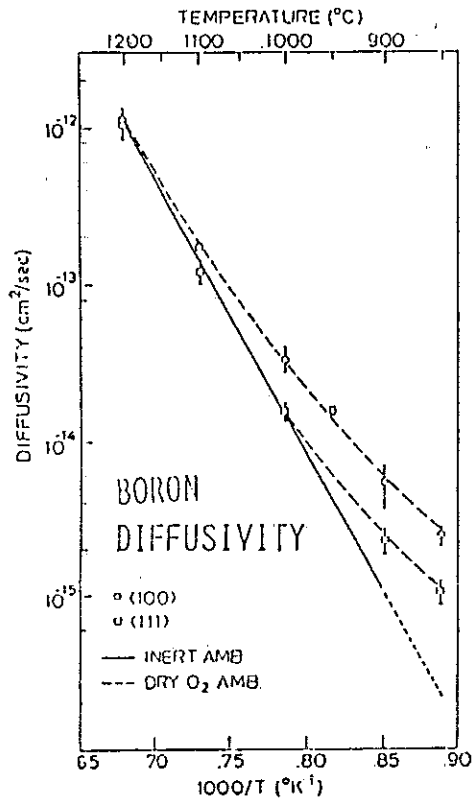
The free volume necessary for the reaction to continue can be supplied by viscous flow or a flux of silicon away from the interface in the form of point defects.

As we noted before, expansion in the plane of the interface (and thus viscous flow) is limited by the bonds between the oxide and the substrate.

Thus, not all the free volume can be provided via viscous flow. The injection of interstitials or annihilation of vacancies are equivalent and can provide the necessary free volume at the interface



Oxidation enhanced diffusion is largest for phosphorus and boron and is most important at lower temperatures.



(LIN, ET AL.)

Oxidation enhanced diffusion has been observed to be dependent on the oxidation rate. (Faster oxidation  $\Rightarrow$  Greater OED)

However, the dependence is sublinear and historically, the data has been fit to an expression of the form

$$C_I - C_I^* = K \left( \frac{dx_o}{dt} \right)^n \quad (1)$$

This expression is also what is used in SUPREM IV.

Usual values of  $n$  are in the range  $0.3 < n < 0.6$ , although values from 0.15 to 1.0 have been reported.

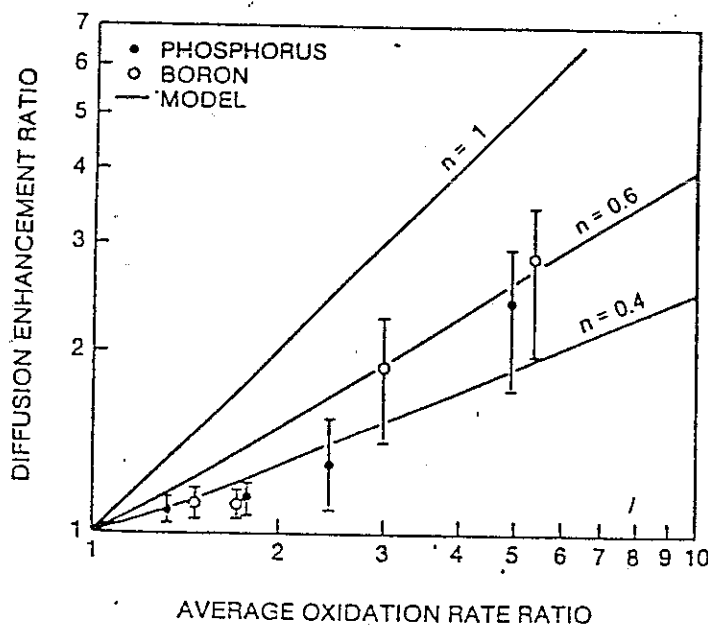
There are many explanations which have been proposed to justify the use of the power-law expression (non-stoichiometric reaction, non-linear interface regrowth, non-linear viscous flow).

Let's approach the problem from a basic modeling perspective.

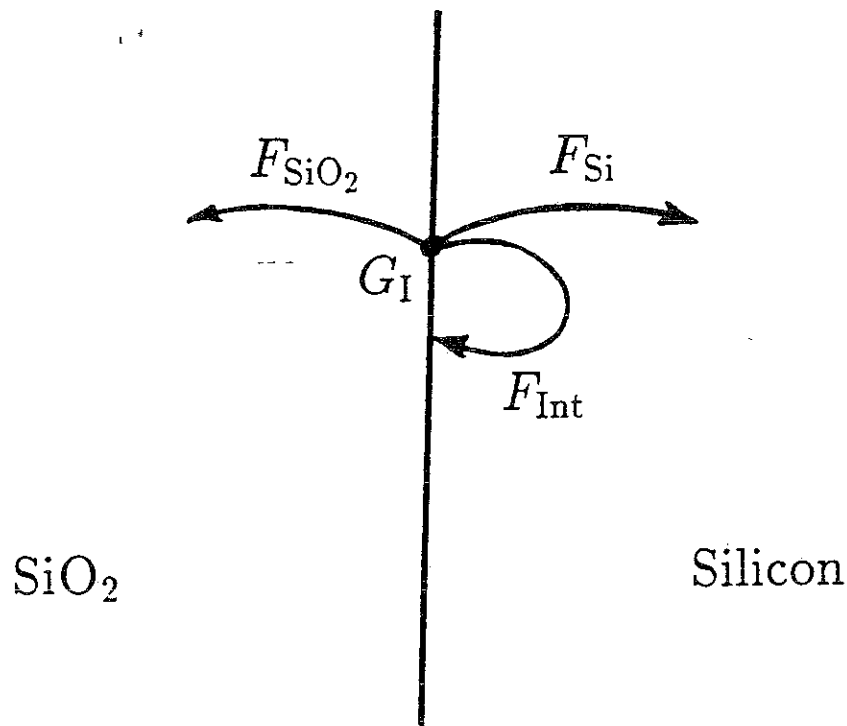
The basic processes are:

- Diffusion of oxidant through oxide.
- Interface oxidation reaction which generates interstitials and annihilates vacancies.
- Segregation of excess silicon (interstitials) between silicon and oxide.
- Flux of interstitials into oxide and silicon and flux of vacancies from silicon.

The point defect concentrations near the interface depend on the balance between interface generation and net flux of silicon in the form of point defects away from interface.



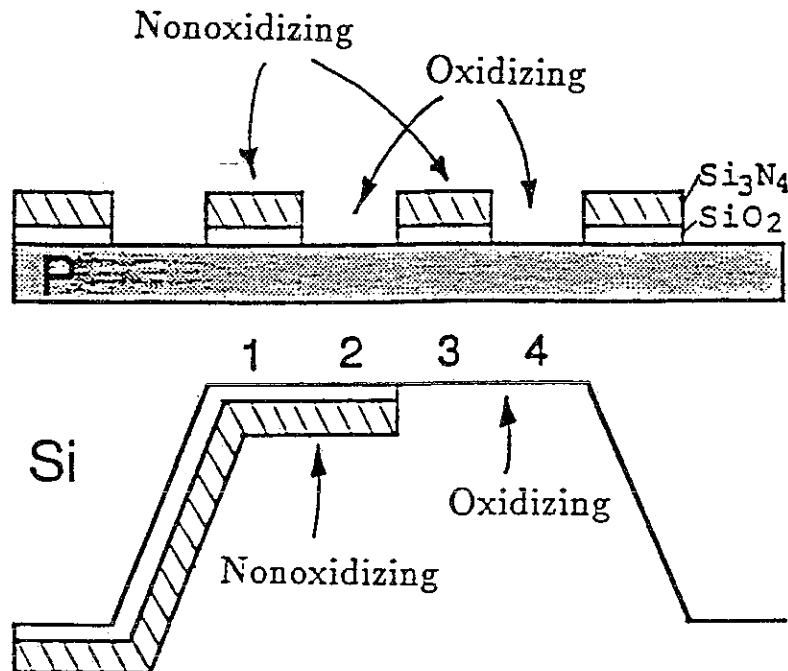
## Interstitial Fluxes



- Interface is source of silicon interstitials ( $G_I$ ).
- Three possible sinks for interstitials:
  - Silicon ( $F_{Si}$ )
  - Oxide ( $F_{SiO_2}$ )
  - Interface ( $F_{Int}$ )
- Changes in dominant sink will alter supersaturation.

# OED in Silicon Membranes

(Ahn, Shott and Tiller)

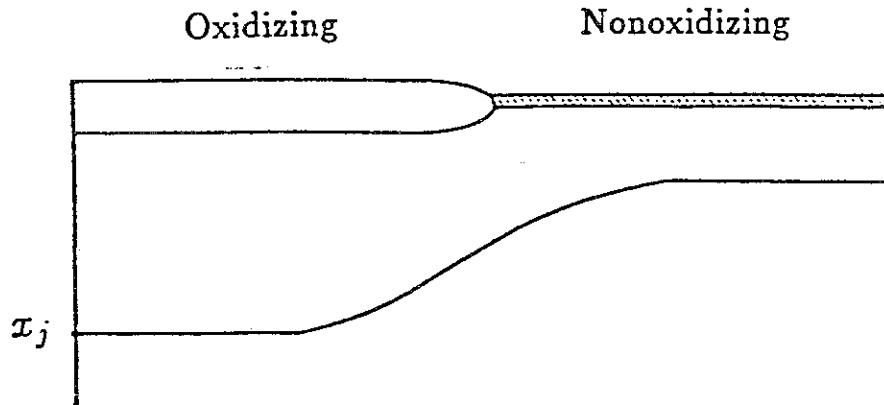


- Diffusion near nonoxidizing interfaces (1,3) strongly enhanced by backside oxidation.
- Diffusion near oxidizing interfaces (2,4) unaffected by backside conditions.
- The oxidation process fixes the interstitial concentration not the flux into the silicon.
- Diffusion into silicon is not dominant sink for interstitials.

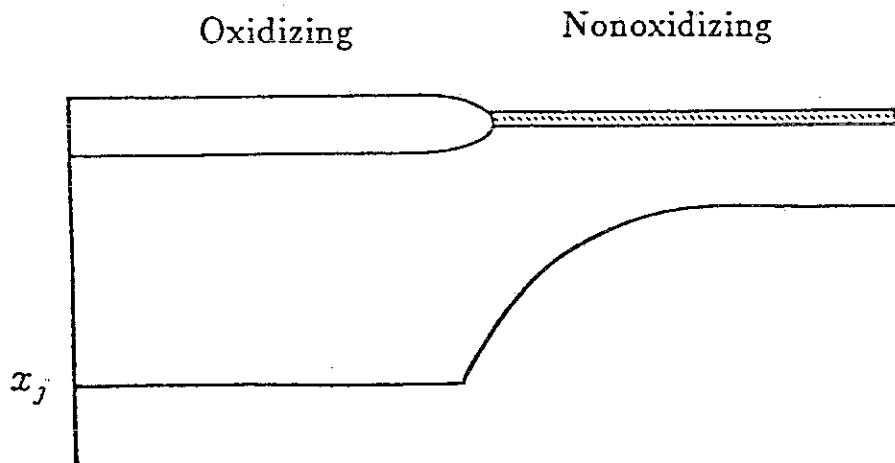
# OED in Two Dimensional Structures

(Griffin and Plummer)

If flux into silicon is important:



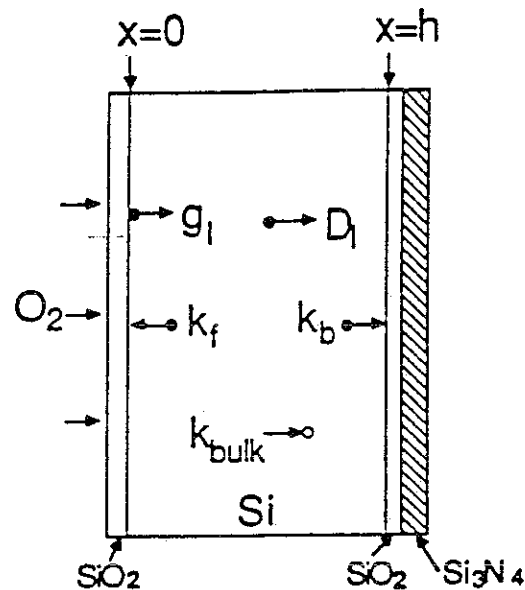
If flux into silicon is negligible:



- Full OED observed up to edge of oxidizing region.
- Diffusion into silicon is **not** dominant flux.
- Reactions at interface and in oxide determine supersaturation.

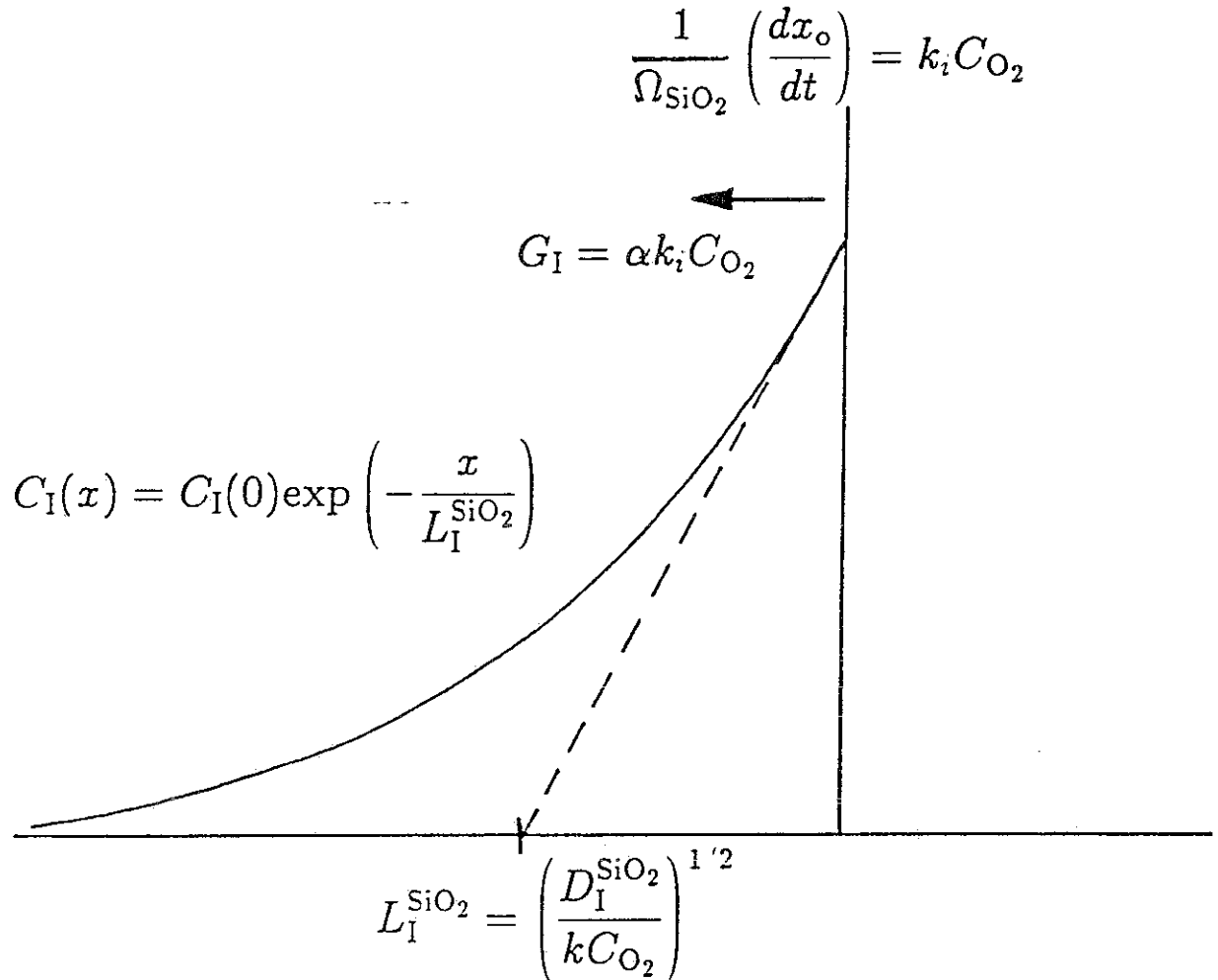


# Interface Regrowth



- To match experimental observations, recombination at the oxidizing interface ( $k_f$ ) must be much larger than at the nonoxidizing interface ( $k_b$ ).
- This is inconsistent with oxidizing interface being the **source** of interstitials.
- Interface regrowth is not primary sink for interstitials.

# Modeling Interstitial Supersaturation



- Interstitials react with oxygen in oxide.
- Generation equals flux into oxide.

## Dependence of Interstitial Supersaturation on Oxidation Rate

$$C_I^{\text{Si}}(0) = m_I \alpha \left( \frac{k_i}{D_I^{\text{SiO}_2} k \Omega_{\text{SiO}_2}} \right)^{1/2} \left( \frac{dx_o}{dt} \right)^{1/2}$$

- The sublinear dependence of interstitial supersaturation on oxidation rate is a consequence of diffusion back into the oxide.
- No assumptions of nonlinearity are required.
- Total concentration, not excess, determined by interface.
- Retarded diffusion possible for very slow oxidation. (Dobson)

## Assumptions

- Sublinear dependence of linear rate constant on  $O_2$  pressure due to two active oxidizing species, one molecular, one atomic:

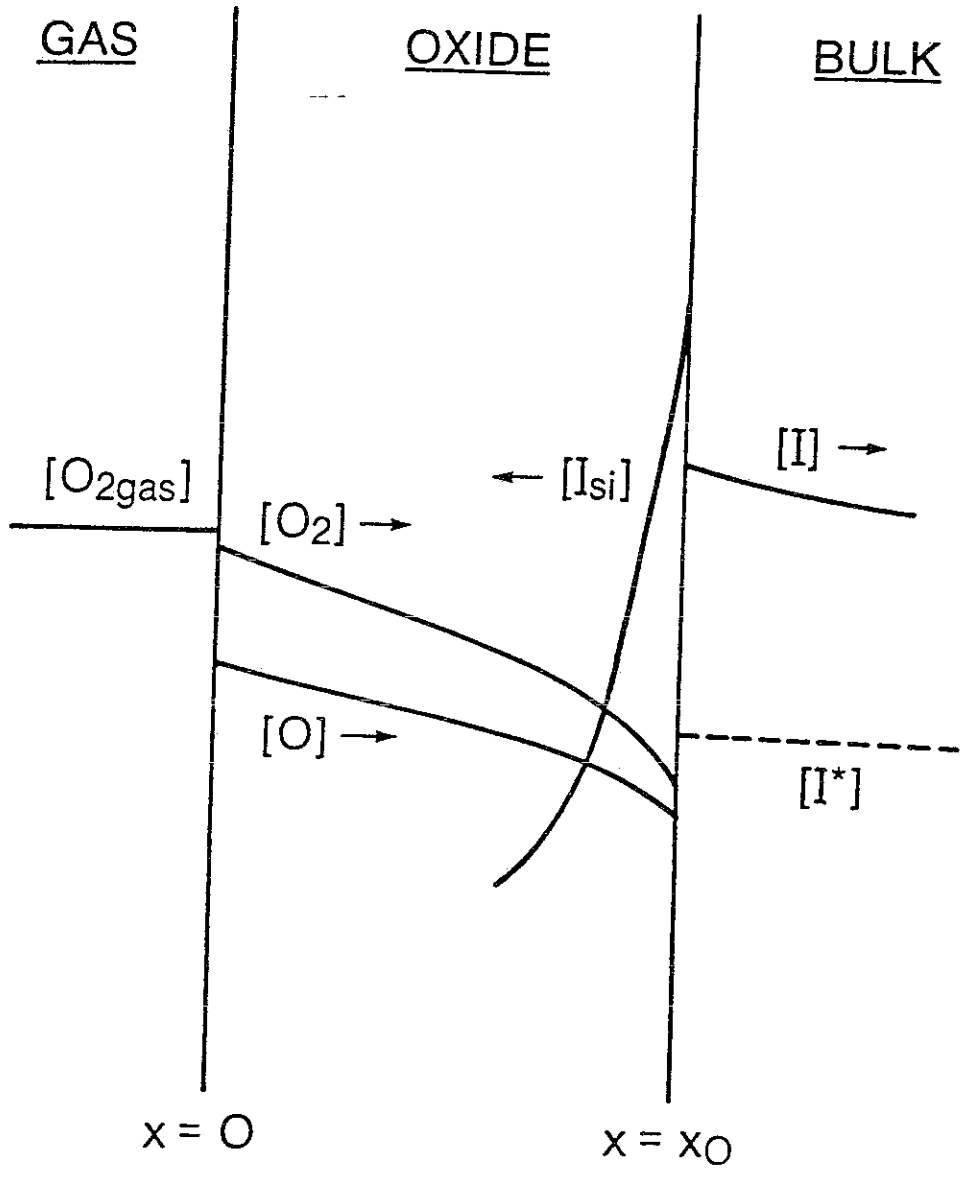
$$\frac{B}{A} \propto p_{O_2}^n, \quad 0.5 < n < 1.0$$

- Relative concentrations of the two species are near equilibrium:

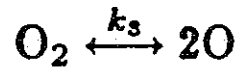
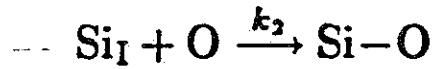
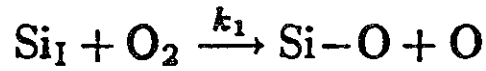


- A fraction of the interface oxidation reactions result in interstitial generation.
- The dominant diffusing species is molecular:

$$B \propto p_{O_2}$$



In oxide:



Continuity equations:

$$\frac{\partial C_{\text{O}_2}}{\partial t} = D_{\text{O}_2} \frac{\partial^2 C_{\text{O}_2}}{\partial x^2} - k_1 C_I C_{\text{O}_2} - k_3 C_{\text{O}_2} + k_{-3} C_{\text{O}}^2$$

$$\frac{\partial C_{\text{O}}}{\partial t} = D_{\text{O}} \frac{\partial^2 C_{\text{O}}}{\partial x^2} + k_1 C_I C_{\text{O}_2} - k_2 C_I C_{\text{O}} + 2k_3 C_{\text{O}_2} - 2k_{-3} C_{\text{O}}^2$$

$$\frac{\partial C_I}{\partial t} = D_I \frac{\partial^2 C_I}{\partial x^2} - \frac{1}{2} k_1 C_I C_{\text{O}_2} - \frac{1}{2} k_2 C_I C_{\text{O}}$$

In steady-state:

$$\frac{\partial C_I}{\partial t} = \frac{\partial C_{\text{O}_2}}{\partial t} = \frac{\partial C_{\text{O}}}{\partial t} = 0$$

Applying boundary conditions, simplifying and solving for  $C_I^{\text{Si}}(x_o)$ :

$$C_I^{\text{Si}}(x_o) = \frac{K_1 \left( \frac{dx_o}{dt} \right)}{\left( 1 + K_2 \frac{dx_o}{dt} \right)^{1/2} - 1},$$

Where,

$$K_1 = m_I \left( \frac{4\alpha}{(1+2\alpha)\Omega} \right) \left( \frac{k_{-3}}{k_3} \right)^{1/2} \left( \frac{2}{k_1 D_I} \right)^{1/2} \left( \frac{k_1^i}{k_2^i} \right)$$

$$K_2 = \left( \frac{4}{(1+2\alpha)\Omega} \right) \left( \frac{k_{-3}}{k_3} \right) \left( \frac{k_1^i}{(k_2^i)^2} \right).$$

$\alpha$  = The percentage of interface reactions that result in interstitialcy creation.

$m_I$  = Si/SiO<sub>2</sub> interstitialcy segregation coefficient.

## Dependence of Model Parameters on Processing Conditions

$K_2$ :

$$K_2 = \left( \frac{4}{(1 + 2\alpha)\Omega} \right) \left( \frac{k_{-3}}{k_3} \right) \left( \frac{k_1^i}{(k_2^i)^2} \right)$$

- Depends on the relative importance of the interface reaction involving molecular oxygen to that involving atomic oxygen.
- Can be calculated from experimental data for the dependence of linear oxidation rate on partial pressure of  $O_2$ .

$K_1/(K_2)^{1/2}$ :

$$\frac{K_1}{(K_2)^{1/2}} = m_I \alpha \left( \frac{4}{(1 + 2\alpha)\Omega} \right)^{1/2} \left( \frac{2k_1^i}{k_1 D_I} \right)^{1/2}$$

- $m_I$  and  $\alpha$  will vary with silicon orientation.
- Depends on the interface reaction rate and the diffusion length for silicon interstitialcies in the oxide.



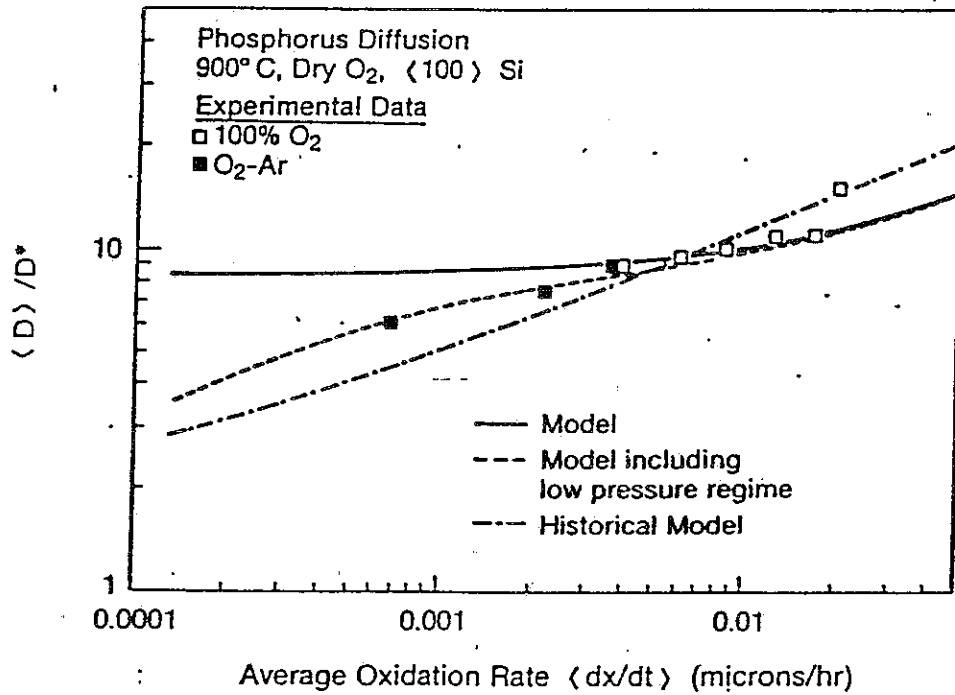


FIG. 10. Diffusion enhancement ratio for phosphorus in <100> silicon vs average oxidation rate for oxidation in dry O<sub>2</sub> at 900 °C in various O<sub>2</sub> concentrations in O<sub>2</sub>-Ar mixtures.

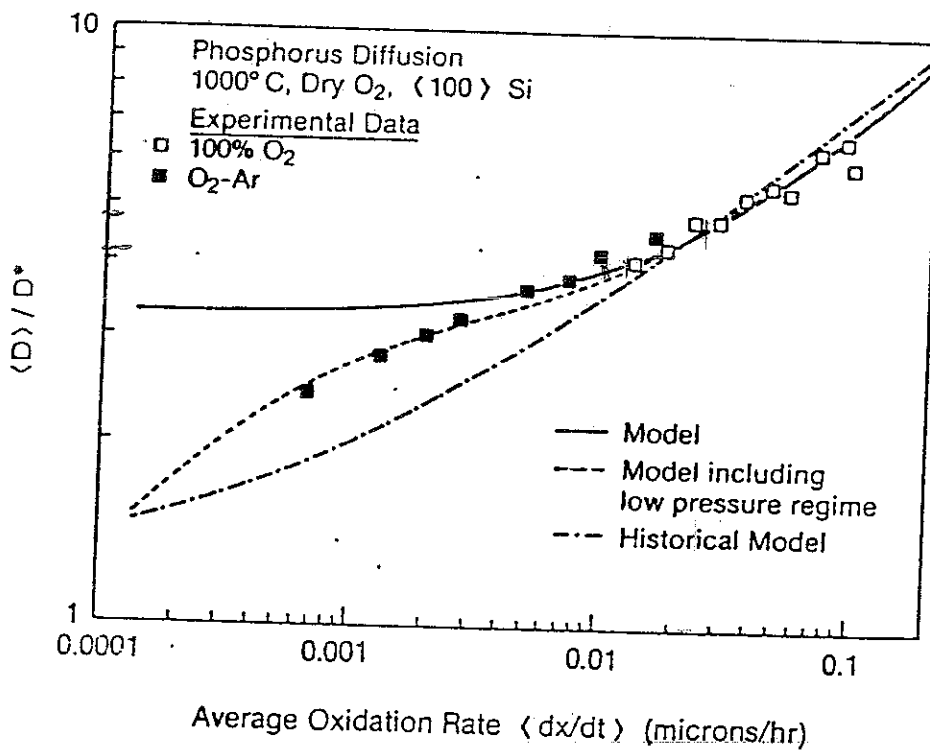


FIG. 11. Diffusion enhancement ratio for phosphorus in <100> silicon vs average oxidation rate for oxidation in dry O<sub>2</sub> at 1000 °C in various O<sub>2</sub> concentrations in O<sub>2</sub>-Ar mixtures.

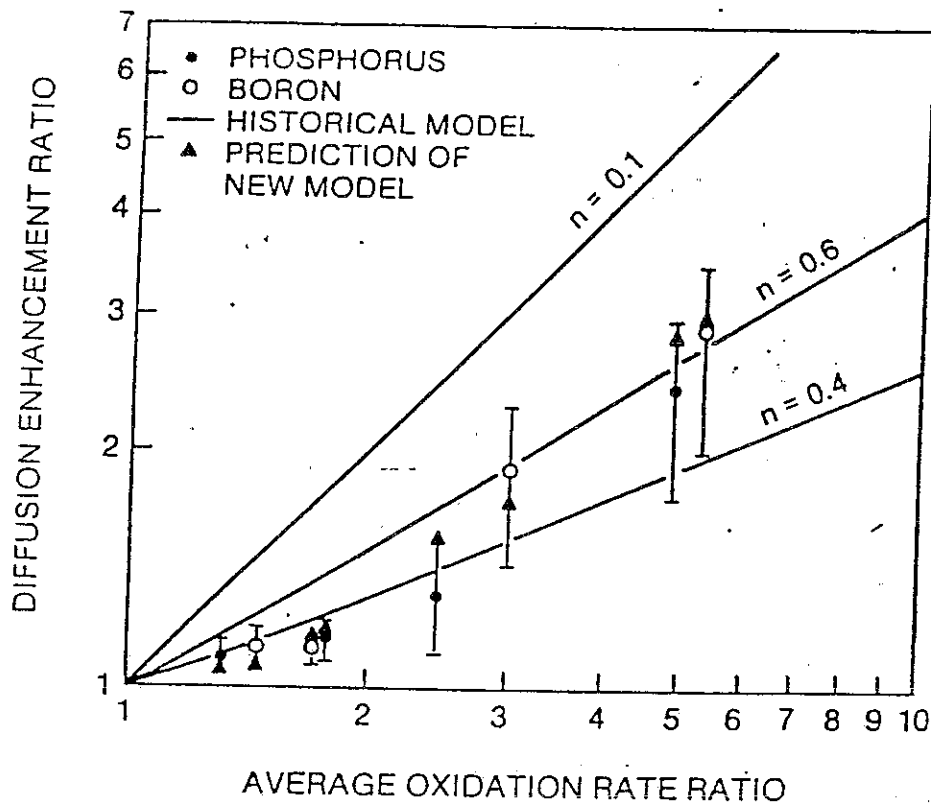
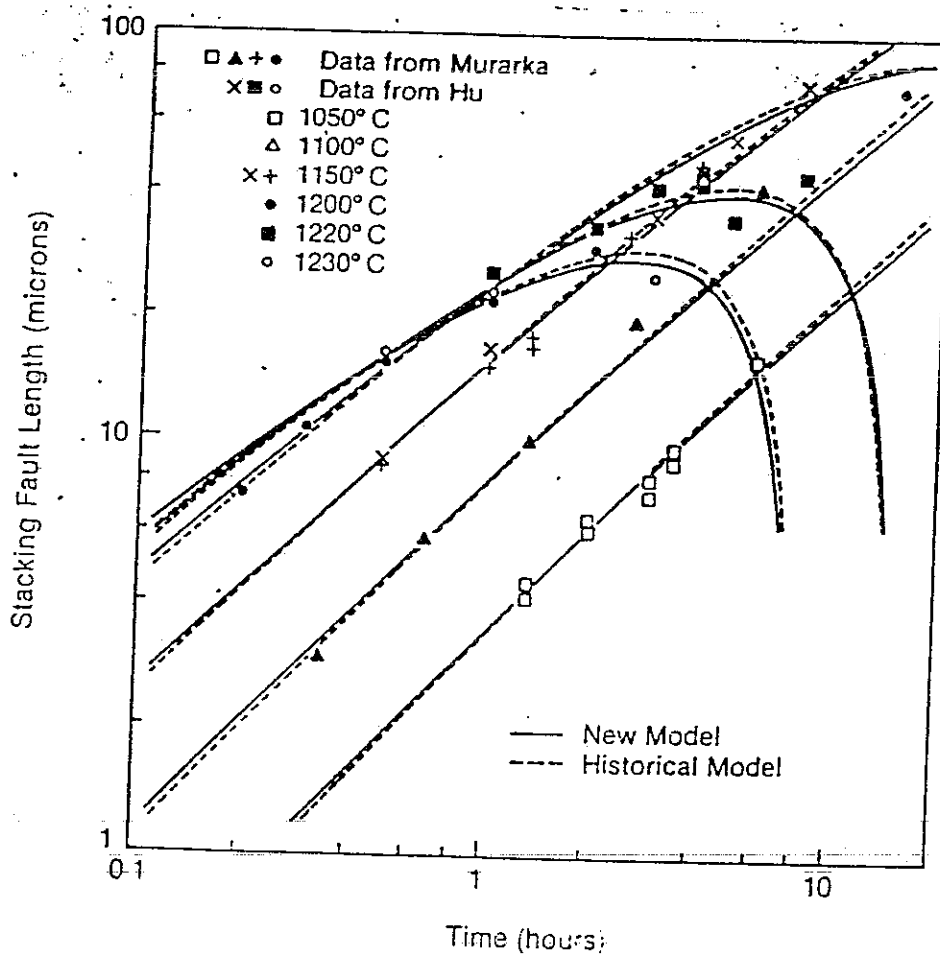
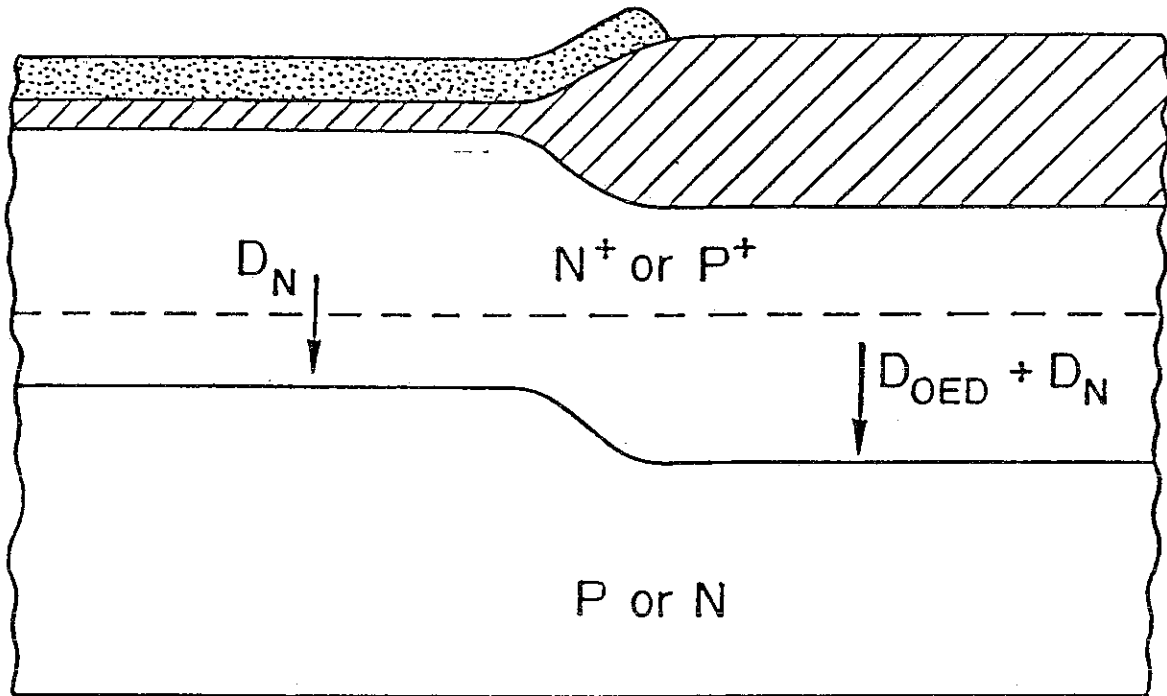


FIG. 14. Predictions and experimental data for the ratio of diffusion enhancements for phosphorus and boron in  $\langle 100 \rangle$  silicon vs ratio of oxidation rates at 900–1200 °C.<sup>3</sup>



# Enhanced Diffusion in Highly-Doped Material



(TANIGUCHI et. al.)

